Measurements of double differential fragment production cross sections of silicon for 70 MeV protons

M. Hagiwara, T. Oishi, S. Kamada, M. Baba,
Cyclotron and Radioisotope Center, Tohoku University
E-mail: *hagi@cyric.tohoku,ac,jp*
T. Sanami
High Energy Accelerator Research Organization (KEK)
M. Takada, N. Miyahara
National Institute of Radiological Sciences

Double-differential fragment production cross-sections of silicon are measured for 70 MeV proton with a specially designed Bragg curve counter (BCC). New method for particle identification and energy correction of range over fragments are applied to BCC and succeed in extension the energy dynamic range. The experimental results of double-differential cross-sections for Li, Be, B, C, N, O production are obtained at 30, 60, 90, 135 degree. The comparisons between the experimental data and theoretical calculations with different models clarified strong dependence of the fragment production on the intra-nuclear cascade model used in calculation.

1. INTRODUCTION

Single Event Effect (SEE) which is a radiation effect induced on a micro-electronics device by hitting of a single ion originated in cosmic radiation has been recognized as a serious problem which disturb the reliability of space technologies. Recently, with miniaturization of a micro-electronics device, SEE becomes a serious problem even on the ground level where there are terrestrial cosmic-rays composed mainly of secondary neutrons created by nuclear spallation reaction in the atmosphere. The most of SEE phenomena induced on the ground is caused by large LET (Linear Energy Transfer) secondary particles produced by the nuclear reaction in a device with the neutrons.

To analyze the SEE mechanism, information on the energy-angular double-differential cross-sections (DDX) of silicon which is main element of a semiconductor device are essential for secondary charged particles productions, especially for large LET secondary particles (called fragment thereafter) by ten's of MeV neutron. However, at present, there are no experimental DDX data for fragment production of silicon in ten's of MeV. Thereby theoretical models for fragment production DDXs have not been examined at all. It is important to accumulate reliable experimental DDX data for fragment production in ten's of MeV.

DDX data for neutrons are of prime importance to estimate SEE on the ground level. However the data are difficult to measure because an intense mono-energetic neutron source enough for the measurements of secondary fragment production which have usually very low cross-section (~ μbarn) is not available in ten's of MeV. To give information about fragment production reaction by ten's of MeV nucleon, DDX data for protons is useful in place of the data for neutrons In the case of a proton experiment, beam intensity is enough to adopt the experiment. Our group has conducted the measurement of the DDX for fragment production reaction by proton using a Bragg curve counter (BCC) [1,2] and Energy Time-of-Flight (E-TOF) method [3,7]. In the previous study [4], DDXs were obtained for the C(p,x) and the Al(p,x) reaction (E_p = 70 MeV) with the BCC and E-TOF method.

The present study aims to obtain DDX of silicon for 70 MeV proton. To improve energy dynamic range of DDX, new methods for particle identification and utilization of range over fragment are described. As a

result, DDXs for fragment production are obtained wide energy range. The DDXs by theoretical calculation with various models are compared with experimental data.

2. BRAGG CURVE COUNTER (BCC)

The details of Bragg curve counter (BCC) are described in the previous report [4]. The BCC is a cylindrical gridded ionization chamber [5,6] (300 mm ϕ x 360 mm long) filled with an Ar + 10%CH_4 gas at a pressure of ~200 torr. A fragment is identified from the transition of the anode signal which reflects the distribution of free electrons produced by the fragment. Since the distribution represents Bragg curve proper to the fragment, the fast part and the whole integration of the signal are proportional to the atomic number (Z) and energy of the fragment, respectively. The energy region which can be measured by the BCC (energy dynamic range) depends on gas pressure of detector and a species of fragment. The high energy limit is determined by maximum stopping energies in detector. In present detector configuration, the maximum stopping energies is 25 MeV for Beryllium, however maximum energy of Beryllium from 70 MeV proton induced reaction reaches 40 MeV. On the other hand, a fragment with energy lower than the energy of Bragg peak can not be identified because Bragg peak information is not included in the anode signal. The energy reaches more than 10 MeV for the fragments heavier than Carbon.

In this study, two new approaches are adopted to extend the energy dynamic range: 1) new identification scheme using a fragment range in place of Bragg peak, and 2) utilization of fragments which penetrate through BCC. For 1), the cathode electrode of BCC is designed to obtain the timing pulse which gives the timing of a fragment entering BCC. Since the anode signal gives the timing of free electron reaching at gird as shown in Fig.1, the time difference between the cathode and the anode shows inverse proportion to fragment range. By using the range, fragment can be identified with any energy, in principle. Thus, the threshold for particle identification is improved considerably. Besides, this method allows identification of not only Z number but also mass number. For 2), the energy of the fragment which penetrated through BCC is estimated from deposition energy in BCC. The relationships between deposition energy and incident energy are calculated by SRIM code for each fragment. The schematic view of this method is shown in Fig. 2. By combining these two approaches, the energy dynamic range of BCC covers almost all the energy of fragments from 70 MeV proton induced reactions.

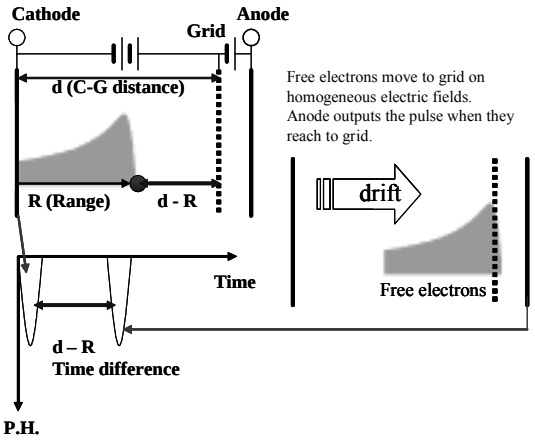

Fig.1. Schematic view of fragment identification from the time difference between the cathode and anode signal

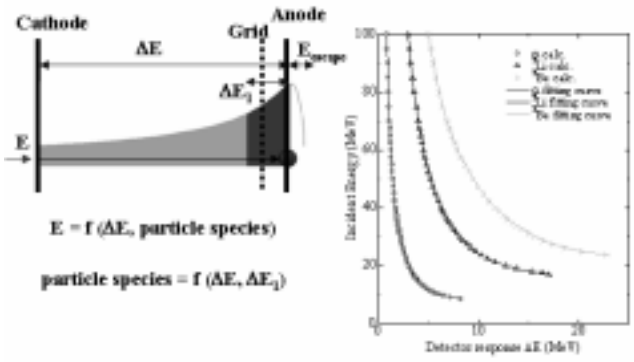

Fig.2. Detection scheme of particle which have the range longer than the detector length.

3. EXPERIMENTS

The experiment are performed using the AVF cyclotron at National Institute of Radiological Science (NIRS) with almost same apparatus as one employed in the previous measurement [4]. The silicon target of 310 μg/cm^2 thick, which is deposited on a tantalum foil of 10 μm thick, is set at the center of a vacuum chamber and irradiated by 70 MeV proton beam with ~30 nA. The effects of the tantalum foil are eliminated by subtracting background data obtained with a tantalum foil without silicon. The fragments from the targets are measured with BCC at 30, 60, 90, 135 degree. Owing to large solid angle of BCC, only 1 hour irradiation is enough for each measurement. At 30 degree, a counter telescope consisted of two SSD (25 μm and 250 μm thickness) and 900 mm flight path is also employed to measure fragments based on E-TOF method. The results of E-TOF are used to evaluate the validity of BCC data.

Figures 3 and 4 show two-dimensional spectra on the energy *vs.* Bragg peak for silicon sample (Si (310 μg/cm^2) + Ta (10 μm)) and backing sample (Ta (10 μm)), respectively. Excellent separation of each fragment and S/N ratio are confirmed up to Z = 8 (Oxygen) for silicon sample in the energy region where particles are separated by the difference of Bragg peak value. As shown in Fig.4, background fragments heavier than lithium are less than 10 % compared with the foreground yields owing to the low fragment production cross-sections of tantalum. Identifications of the fragments were also performed by time difference between cathode and anode signals as shown in Fig 5 and the performances of two methods (Bragg peak and time difference method) are compared. As the results, identification with a time difference is better than with a Bragg peak on the point of lower energy limit to identify each fragment and isotope identification.

The turning blows at maximum energy point in Fig. 3 and 4 are caused by the fragments which have ranges longer than the cathode-grid distance (300 mm) which is the detector active region. In the past BCC method, the events were excluded from the energy spectra because the fragments are not fully deposit the energy to the detector and therefore become limitations of measurable detector energy in high energy. It is meaningful to extend the measurable energy range by developing a correction method for this effect from the information of the partial energy deposit (ΔE) In this study, the energy dynamic range of fragments was extended by introducing the energy correction method with the relation of E (energy which fragments have before the injection to detector) and ΔE (energy which fragments give to detector) calculated by SRIM code.

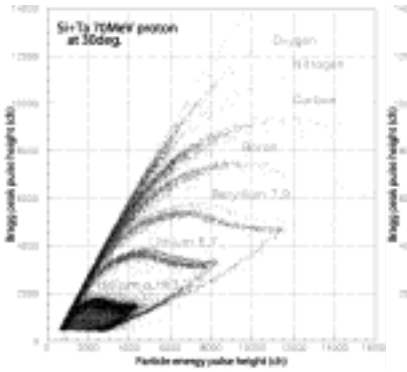

Fig.3 Two dimensional spectrum of energy *vs.* Bragg peak for silicon sample

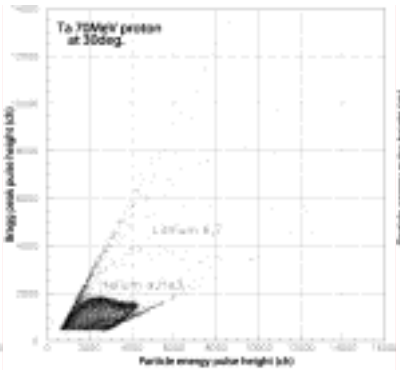

Fig.4 Two dimensional spectrum of energy *vs.* Bragg peak for tantalum backing

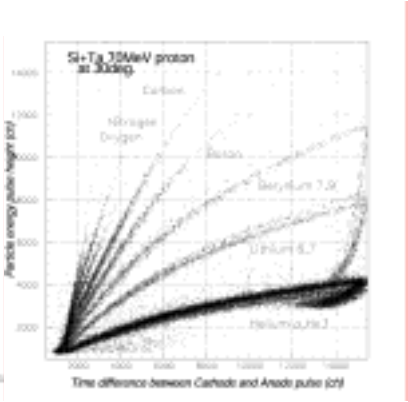

Fig.5 Two dimensional spectrum of time difference vs. energy for silicon sample

4. RESULTS AND DISCUSSION

Figure 6 shows the comparison of beryllium spectra with and without the energy correction for range over particle for example. The dynamic range of beryllium was extended reasonably by the corrections from around 25 to 38 MeV which is close to a kinematics maximum energy of beryllium.

Figure 7 shows the comparison between experimental data by BCC and ETOF with LA150[9]. The data by BCC are consistent with one by E-TOF in the overlapping region and are also consisted with one by LA150 which have been examined by another experiment. These facts confirm the method for absolute normalization and energy calibration of the data by BCC.

Figure 8 shows the Li, Be, B, C, N, O production double-differential cross-sections of silicon for 70 MeV proton at 30, 60, 90, 135 degree with the results of PHITS [10] calculations. The calculations carried out using three different intra-nuclear cascade models (ISOBAR, JQMD, Bertini) combined with one evaporation model (GEM). Considerable amount of fragments whose energy reaches to 20 MeV are observed as the results of 70 MeV proton induced reaction. The threshold energies of experimental data are determined from the thicknesses of sample and incident window. These thicknesses can be improved by the experimental setup focused at low energy fragments. The ISOBAR model generally reproduces experimental data except for the data of light fragments. The calculations with Bertini model show remarkable underestimates for all results. Therefore, to calculate correct deposition energy by a code in this energy range, we should pay much attention what model embedded in the code. At forward angle of lithium and beryllium DDXs, the experimental data show a different shape from the other data. This fact indicates that a new reaction mechanism is indispensable to reproduce these components. For the experimental data of ^{7}Be production cross-sections [12] and mass distribution [7] in this energy region, ISOBAR model underestimate the data, the discrepancies of which are similar trends for the present results as shown in Fig. 9. The models will be required for the improvements of the light cluster treatments to improve the calculation accuracy.

Figure 10 shows the comparison between DDXs of silicon and aluminum for He, Be, C and O at 30 degree. The magnitude and shape of fragment DDXs of aluminum are in good agreement with ones of silicon which are similar results in Fig. 9. Thus, the data of silicon can be estimate from ones of aluminum which can be obtained using a self-support sample. From an experimental point of view, it is important because a sample of aluminum is easy to fabricate in comparison with one of silicon.

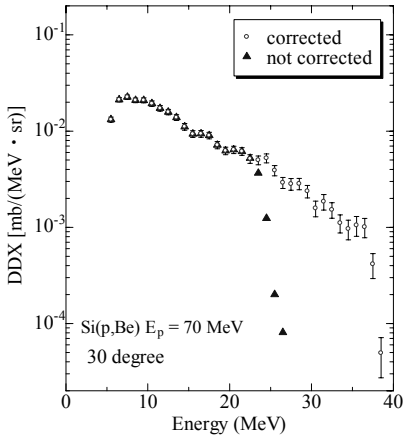

Fig.6 Comparison of beryllium spectra with/without the energy correction for range over events

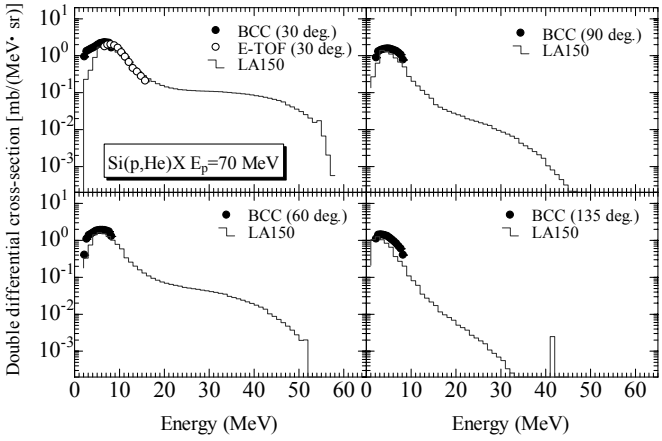

Fig.7 Comparison of DDX of Si(p,α) (Ep = 70 MeV) with LA150

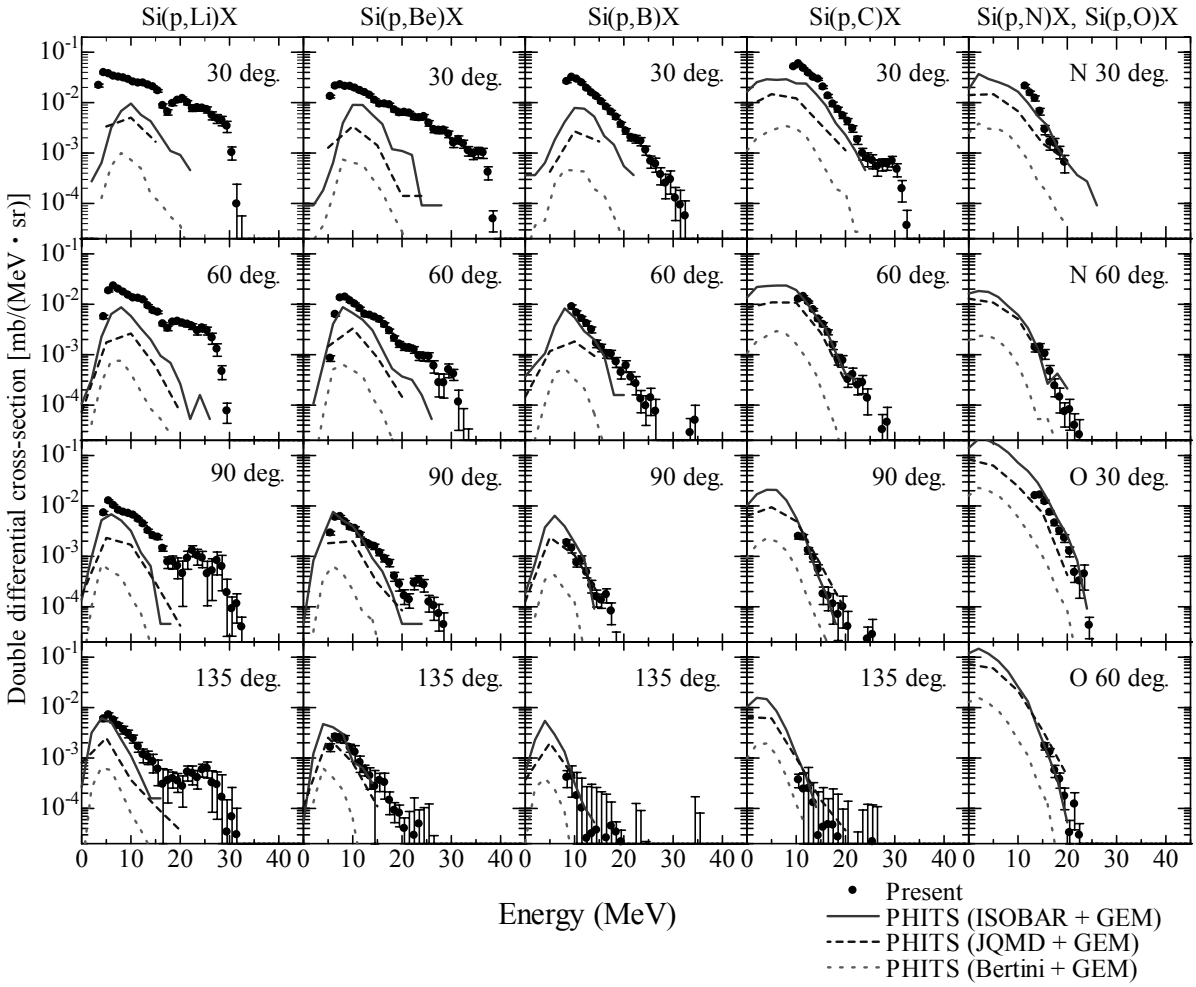

Fig.8 DDX of silicon for Li, Be, B, C, N, O production at 30, 60, 90, 135 degree from for 70 MeV proton reaction compared with the results of PHITS [10] calculations

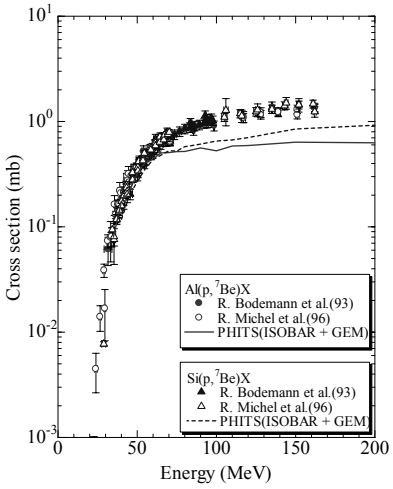

Fig.9 ^{7}Be production cross-section [11,12] of Si and Al compared with PHITS

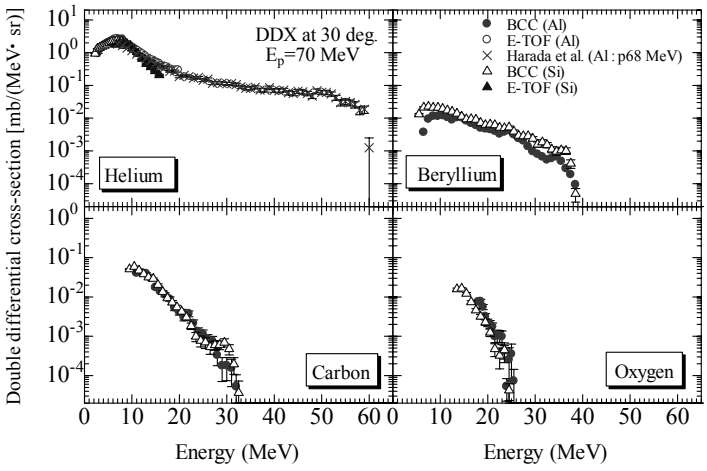

Fig.10 Comparison between DDXs of silicon and aluminum for He, Be, C and O at 30

5. CONCLUSION

Fragment production double-differential cross-sections of silicon for 70 MeV proton induced reaction are obtained using a specially designed BCC. The energy dynamic range of BCC is extended remarkably by a new identification scheme using particle range and a utilization of particles whose ranges are longer than the detector. The α-particle production double-differential cross-section data by the new methods are consistent with the data by E-TOF method and LA150. It becomes clear that considerable amount of fragments whose energy reaches to 20 MeV are produced from the Si(p,x) reaction in tens MeV region. By the comparison with theoretical calculations, the applicability of the calculation for fragment productions strongly depends on the model of an intra-nuclear cascade part. The ISOBAR model generally reproduces experimental data except for the data of light fragments. To reproduce these light fragment productions, a new reaction model will be indispensable. The comparison between results obtained with aluminum and silicon sample show that aluminum have similar DDXs for fragment production and can be substituted for silicon.

Our data will play important role in estimation of radiation effects on a silicon based semiconductor devices since this data set is only one data which describes fragment production rate and the energy spectra in this energy range. The data will be useful for not only benchmark data for the fragment production but also estimation of local charge density by proton in silicon. This data will be also useful for the estimation of neutron induced reaction by taking account of the coulomb contribution in the nuclear reaction.

ACKNOWLEDGEMENT

The authors express their thanks to the operation crew of the NIRS cyclotron for their cooperation. The authors wish to thank Dr. Sugai of KEK for his effort in fabrication of silicon samples with HIVAP method.

REFERENCES

[1] C.R.Gruhn, M.Binimi, R.Legrain, R.Loveman, W.Pang, M.Roach, D.K.Scott, A.Shotter, T.J.Symons, J.Wouters, M.Zisman, R.Devries, Y.C.Peng and W.Sondheim, Nucl. Instrum. Methods, 196 (1982) 33

[2] N.J.Shenhav and H.Stelzer, Nucl.Instrm.Meth. 228 (1985) 359

[3] C.T.Roche, R.G.Clark, G.J.Mathews and V.E.Viola, Jr, Phys. Rev. C 14 (1976) 410

[4] M. Hagiwara, T. Sanami, M. Baba, T. Oishi, N. Hirabayashi, M. Takada, H. Nakashima and S. Tanaka, Proc. of the international conference on Nuclear Data for Science and Technology ND2004, 769 (September 2004) 1031.

[5] T. Sanami, M. Baba, M. Hagiwara, T.Hiroishi, M.Hosokawa, N.Kawata, N.Hirabayashi, T.Oishi, H.Nakashima and S.Tanaka. J. Nucl. Sci. and Tech. Suppl. 4 (2004) 502

[6] T.Sanami, M.Baba, K.Saito, N.Hirakawa. Nucl. Instrum. Meth. A440 (2000) 403

[7] K. Kwiatkowski, S. H. Zhou, T. E. Ward, et al., Phys. Rev. Lett. 50 (1983)1648

[8] K.Omata and Y.Hujita, INS-Rep-884, Institute for Nuclear Study, University of Tokyo, 1991

[9] M. B. Chadwick, P. G. Young, S. Chiba, S.C. Frankle, G. M. Hale, H. G. Hughes, A. J. Koning, R. C. Little, R. E. MacFarlane, R. E. Praeel and L.S. Waters, Nucl. Sci. Eng., 1331 (1999) 293

[10] H. Iwase, K. Niita, T. Nakamura, J. Nucl. Sci. and Tech. 39 No.11 (2002) 1142

[11] R. Bodemann, H.-J. Lange, R. Michel, T. Schiekel et al., Nucl. Instr. Meth. B82 (1993) 9.

[12] R. Michel, R. Bodemann, H. Busemann, R. Daunke et al., Nucl. Instr. and Meth. B129 (1997) 153